Quantifying growth mechanics of living, growing plant cells in situ using microrobotics

Felekis, D

Abstract: Plant cell growth is a fundamental process during plant development and the developmental biology society has studied cell growth from various aspects using physiological, biochemical, genetic, mathematical and modelling approaches. Recent advances in the field of biology demonstrate a need for investigation and quantification of the mechanics of growth at individual cellular levels. Here, we describe a microrobotic system capable of performing automated mechanical characterisation of living plant cells in situ as these cells proliferate and grow. The microrobotic measurement system employs a single-axis capacitive MEMS microforce sensor, a multi-axis positioning system with position feedback, a high-resolution optical microscope and a custom-user interface for the guiding of the automated measurement process. The system has been applied to measure mechanical properties of Lilium pollen tubes approximately 20–m wide. The measurements were performed in growth medium, and the observed growth rate of the pollen tubes is about 20–m per minute. For the mechanical characterisation of pollen tubes, nano-Newton level loads and nanometric indentations are applied. The force-deformation data obtained show a difference in stiffness from the tip to the apex demonstrating that the developed measurement system is a promising tool for better understanding the mechanics of plant cell growth.

DOI: https://doi.org/10.1049/mnl.2011.0024

Quantitating growth mechanics of living, growing plant cells in situ using microrobotics

Dimitris Felekis[1], Simon Muntwyler[1], Hannes Vogler[2], Felix Beyeler[1], Ueli Grossniklaus[2] and Bradley J. Nelson[1]

1 Institute of Robotics and Intelligent Systems, ETH Zurich, 2 Institute of Plant Biology, University of Zurich

ABSTRACT

Plant cell growth is a fundamental process during plant development and has been an important research topic for many decades. The developmental biology society has studied cell growth from various aspects using physiological, biochemical, genetic, mathematical and modeling approaches. Recent advances in the field of biology demonstrate a need for investigation and quantification of the mechanics of growth at individual cellular levels. Here, we describe a microrobotic system capable of performing automated mechanical characterization of living plant cells in situ as these cells proliferate and grow. The microrobotic measurement system employs a single-axis capacitive MEMS microforce sensor, a multi-axis positioning system with position feedback, a high-resolution optical microscope and a custom user interface for the guiding of the automated measurement process. The system has been applied to measure mechanical properties of Lilium pollen tubes approximately 20 μm wide and 400 μm long. The measurements were performed in an aqueous environment, more specifically in growth medium, and the observed growth rate of the pollen tubes is about 20 μm per minute. For the mechanical characterization of pollen tubes nanoNewton level loads and nanometric indentations are applied. The force-deformation data obtained show a difference in stiffness from the tip to the apex demonstrating that the developed measurement system is a promising tool for better understanding the mechanics of plant cell growth.

1. Introduction

Almost all our food, feed, fuel and fiber are ultimately derived from plants. Additionally, photosynthetic organisms have a major impact on the global climate since they

comprise 99% of the earth's biomass. To this end, understanding the growth process and how plants interact with their natural environment during growth is fundamental.

Plant development is the result of three essential processes: cell expansive growth, cell division and cellular differentiation. Cellular expansive growth is one of the foundations of morphogenesis that involves changes to cellular size and shape. In plant cells, because of the presence of the extracellular matrix, these changes require the combined action of two mechanical processes: the deformation of the existing cell wall and the secretion and deposition of new cell wall material [1]. For the precise targeting of the latter process, the role of the cytoskeleton is crucial, whereas turgor pressure supplies the force for the former deformation. However, the dynamics of the growth process as well as the resulting final cell size and cellular shape are controlled by the mechanical behavior of the cell wall [2-6].

Therefore, theoretical and biophysical descriptions of cellular growth processes focus on mathematical models of cell wall biomechanical responses to tensile stresses, produced by the turgor pressure. The values of the input parameters to these models are often based on qualitative knowledge rather than on accurate quantitative descriptions. For the automated mechanical characterization of growing cells at the cellular and sub-cellular level we developed a robotic system that enables the measurement of sub-microNewton forces and sub-micrometer deformations and provides biologically plausible models with accurate quantitative data.

Several technologies have been reported for the characterization of biological materials such as magnetic tweezers [7], optical tweezers [8], atomic force microscopy (AFM) [9-10], substrate stretching [11], micropipette aspiration [12] and MEMS-based devices. Sensing based on magnetic and optical trapping is a technology suitable for biological applications for measuring forces in the pico-Newton range. AFM is a mature technology that has been applied to the life sciences as well. However, due to a limited scanning range, AFMs are only used to characterize areas of hundreds of μm^2 or less. Also, cantilever-based sensors are sensitive to off-axis loads and induce lateral motions when they are deflected, sometimes inducing slippage. Despite the metrological limitations of the cantilever as a force sensor, few viable alternatives exist [13]. MEMS based force sensors have been used for multiple applications in biological research, such as for measuring forces on single heart cells

[14], measuring the injection force on Drosophila embryos [15], studying cell mechanical response [16], characterizing fruit fly behavior and investigation of micromechanical properties of mouse zona pellucida and of soft hydrogel microcapsules [17-19]. These sensors are capable of measuring local properties of biological materials and microfabricated MEMS grippers have been demonstrated for quantifying global mechanical properties [20-22].

Here we use lily (*Lilium longiflorum*) pollen tubes as a model for tip growing cells because it is an organism that plant biologists have long studied and it is easy to cultivate and to harvest. We study pollen tube growth because it is an important process in the sexual reproduction of higher plants. Pollen tube growth is required to deliver male gametes to female reproductive structures. After hydration and germination, pollen tubes grow along the stylar transmitting tract into the ovary, where they finally enter the micropylar openings of the ovules, the precursors of seed. Through the micropylar opening the pollen tube reaches the embryo sac and penetrates an accessory cell (synergid) to release two sperm cells required for double fertilization. To reach the most distal ovules in a pistil the pollen tube must cover a distance that ranges from several millimetres up to 50 cm in maize (*Zea mays*) and requires rapid polar cell expansion along the longitudinal axis. The time window for successful fertilization is relatively short. Lily pollen tubes elongate at a moderate but still amazing rate of about 2 mm/h [23-25]. Since cellular growth is restricted to the tip of the pollen tube, the cell wall in this zone must be deform, whereas in more distal parts (the shank) the main function of the wall is to resist turgor pressure. It has been shown that the composition as well as the mechanical properties of the cell wall differ between the tip and the shank of pollen tubes [1, 26].

The aim of this work is to develop a versatile system capable of characterizing living cells and organisms of highly diverse and changing morphology under different physiological conditions in situ. By automating the measurement procedure we are able to conduct multiple high-resolution stiffness measurements over multiple samples in a small time interval as the organism grows.

In the robotic system described in this paper a microfabricated single-axis MEMS-based capacitive force sensor is used. The FT-S540 microforce sensing end effector that is commercially available from FemtoTools GmbH is mounted on a three-axis positioning

system with integrated position feedback sensor, capable of moving over a range of thirty millimeters and a resolution of five nanometers. A high-resolution optical microscope and a custom user interface are integrated with the positioner/force sensor into a complete microrobotic measurement system.

2. Microforce sensor calibration and characterization

A commercial available capacitive MEMS-based microforce-sensing probe (FT-S540, FemtoToools GmbH) is used for the micromechanical investigations. Event though the sensor is precalibrated by the manufacturer, in order to ensure its suitability, a complete sensor calibration and characterization is performed, as SI-traceable calibration as well as uncertainty analysis characterization for all commercially available microforce sensors remains a topic under investigation.

The working principle of the sensor is schematically shown in Fig. 1. The sensor consists of a movable body with an attached probe suspended by four flexures within an outer frame. A force applied to the probe in the x-direction results in a relative motion of the body and the outer frame, which can be measured by attached capacitive electrodes as a change in capacitance. By measuring two capacitive changes with opposite signs differentially using a capacitance-to-voltage converter integrated circuits (MS3110, Irvine Sensors Inc.), a linear sensor characteristic is achieved.

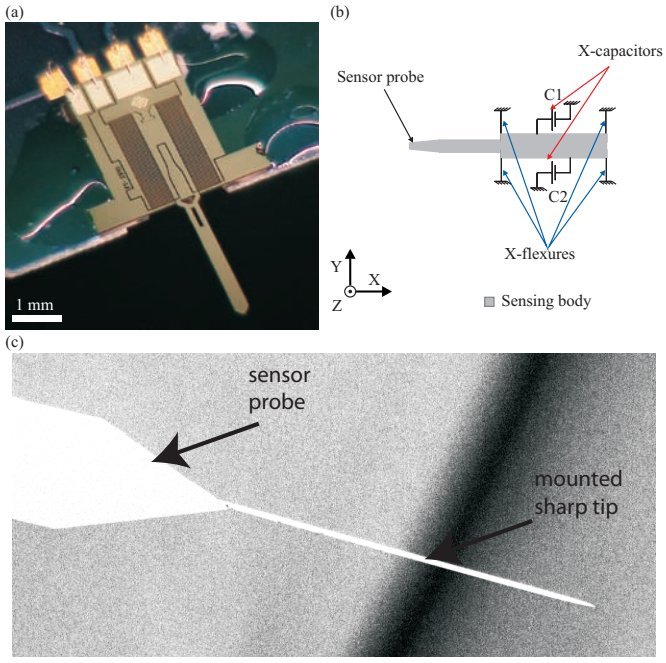

Fig. 1: (a) Photograph, (b) schematic of a single-axis MEMS-based capacitive microforce-sensing probe (FT-S540, FemtoTools GmbH), SEM picture of the MEMS force sensor's tip with the mounted sharp tip of 100nm point radius.

Due to the symmetric design of this sensor with its four flexures, parallel motion of the movable body as it is deflected can be achieved, making this design superior to most cantilever-type sensors. Furthermore, due to its long sensing probe, the sensor can access three dimensional structures, even in depressions.

The most commonly used microforce sensor, the AFM, has led to the development of a large number of methods for calibrating forces in the micronewton and nanonewton range [26]. However, the accuracy of these methods is unknown since most of them are based on a model of the sensor and are, therefore, not SI-traceable resulting in nonquantitative measurement results.

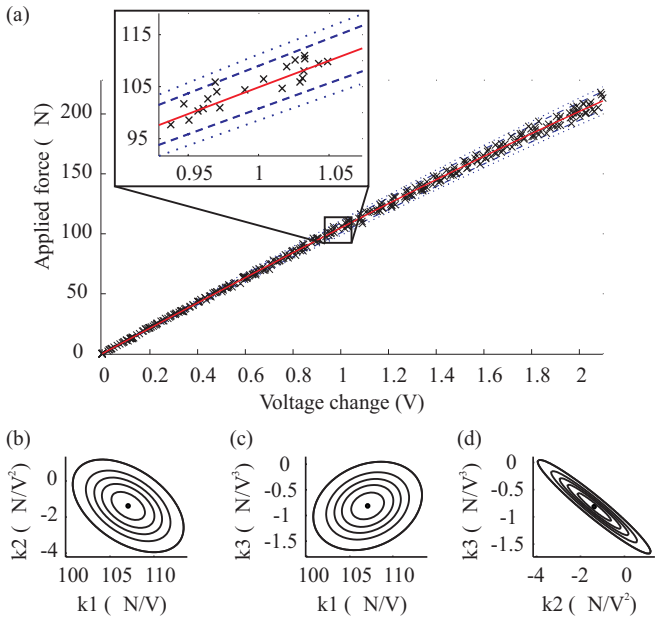

Fig. 2: Calibration results of the single-axis MEMS-based microforce-sensing probe consisting of (a) the calibration data (x) as well as the best estimate (-), the 68% (--), and the 95% (..) coverage interval of the calibration curve, (b) – (d) contour lines of the multivariate PDF of the calibration coefficients for coverage probabilities of 10%, 30%, 50%, 70% and 90%, projected onto the calibration coefficient plane of (b) k1 and k2 (c) k1 and k3 (d) k2 and k3.

To realize traceable microforce measurements in the sub-micronewton range the microforce-sensing probes have been calibrated using a custom built microforce sensor as a

reference that's pushed against the target sensor using a motorized linear stage (MT1-Z6, Thorlabs Inc.). The resulting calibration data is shown in Fig. 2. The reference sensor has been precalibrated using an SI-traceable compensated semi-microbalance (XS205DU, Mettler-Toledo International Inc.) and steel weights as a transfer artifact.

This integration of tools benefits from the high accuracy and mature technology of the precision balance, while eliminating the disadvantage of the slow reaction time and its influence on calibration uncertainty due to signal drift when directly used as a reference.

The result of a measurement or calibration is only an approximation of the value of the measurand and, thus, it is complete only when accompanied by a statement of the uncertainty of that estimate [28]. The measurement uncertainty is a parameter associated with the results of a measurement that characterizes the dispersions of the values that could reasonably be attributed to the measurand [29]. Therefore, for SI-traceability, besides the measurement result, its uncertainty also needs to be measured and propagated throughout the entire calibration chain, starting with the primary reference standard and its uncertainty. For the evaluation and combination of the uncertainties we use the internationally accepted master document, Guide to the Expression of Uncertainties in Measurements (GUM) [28] published by the International Organization for Standardization's (ISO).

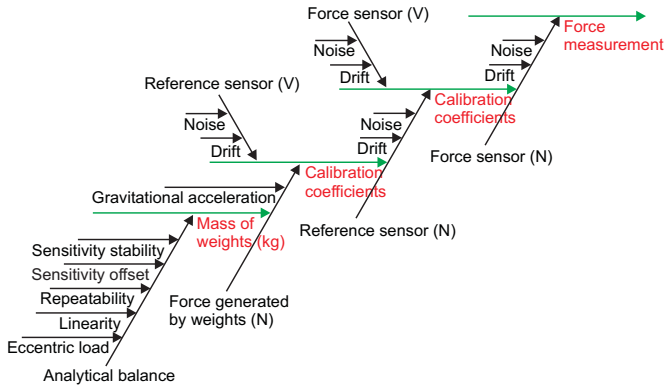

Fig. 3: Cause and effect diagram for the propagation of the diverse sources of uncertainty in the calibration chain.

All the different sources of uncertainty in the calibration chain, shown in the cause and effect diagram in Fig. 3, are evaluated and propagated to the final force measurement of the single-axis microforce sensor. We use the multivariate adaptive Monte Carlo method (MCM) presented in the second supplement to the GUM [30]. All sources of uncertainty are

described by their probability density function (PDF). By randomly sampling from these PDFs and using the method of ordinary least squares, a third-order polynomial function as shown in (1) is fit to the calibration data for each of these Monte Carlo trials, minimizing the residual r_i. These sets of the calibration coefficients (c_1, c_2, c_3) give a discrete representation of the multivariate PDF of the result. From this PDF the best estimate, its standard uncertainties and the correlation and expansion coefficient of the calibration coefficients can be calculated as shown in Table 1.

$$\mathbf{F}_i = \begin{pmatrix} \mathbf{V}_i & \mathbf{V}_i^2 & \mathbf{V}_i^3 \end{pmatrix} \cdot \begin{pmatrix} c_{1,i} & c_{2,i} & c_{3,i} \end{pmatrix}^{\mathrm{T}} + \mathbf{r}_i \qquad \text{for } i = 1 - M \qquad (1)$$

For this resulting multivariate PDF (third order), no coverage interval with only an upper and a lower bound – as is the case with the single variant – can be defined. For three outputs, a coverage volume (ellipsoid) is needed whose contour lines for coverage probabilities of 10%, 30%, 50%, 70% and 90%, are shown in Fig. 2 (b)-(d) as projections onto the calibration coefficient plane. By using this multivariate PDF as input for the uncertainty calculation of the force predictions made with this sensor, the correlation between the coefficients is adequately taken into account. In Fig. 2(a) the calibration data and the best estimate from the least squares fits, as well as the coverage interval for the two coverage probabilities p1 = 68% and p2 = 95% are shown.

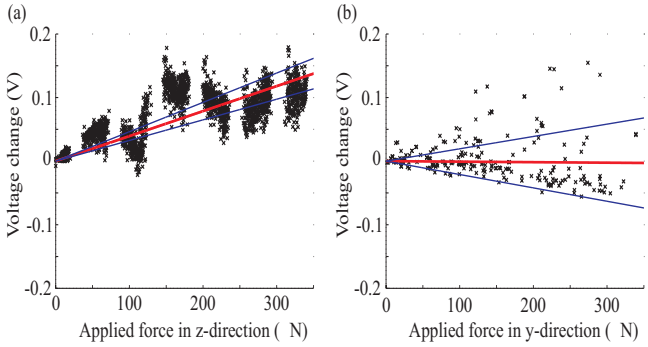

Fig. 4: Cross sensitivity measurement data (x) as well as the best estimate (-) and its standard uncertainty (-) for the applied force (a) in the z-direction and (b) in the y-direction

Besides the parallel motion of the movable body, the four-flexure configuration with the high aspect ratio flexures greatly reduces the cross sensitivity to off-axis forces. To

confirm this assumption, the cross sensitivity of the sensing probes to off-axis forces is measured by calibrating the sensor along the two off-axis directions, the y- and z-directions.

The results shown in Fig. 4 indicate a neglectable cross sensitivity of the sensor to off-axis in-plane forces in the y-direction, and out-of-plane forces in the z-direction. The results demonstrate a high selectivity of the single-axis sensing probe of 26 ± 5.

Table 1: Calibration and uncertainty analysis results: single-axis MEMS-based microforce-sensing probe

Input range *Fx* (mN)	±230
Output range (V)	0 – 4.5
Calibration coefficients (mN/V mN/V^2 mN/V^3)^T	$(107.07\ -1.38\ -0.81)^T$
Standard uncertainties (mN/V mN/V^2 mN/V^3)^T	$(2.52\ 1.02\ 0.34)^T$
Correlation coefficients	
r_{12}	-0.468
r_{13}	0.247
r_{23}	-0.960
Expansion coefficient k_p for	
p1 = 0.68	1.86
p2 = 0.95	2.80
# MCM iterations: *M*	$2.88 \cdot 10^6$
u_{Noise} at 10 Hz (µN) PDF: normal	0.02
u_{Drift} (t = 30s) (µN) PDF: normal	0.07
Selectivity of Fx to Fy	∞
Selectivity of Fx to |Fz|	26 ± 5

The entire set of characteristic parameter of the single-axis microforce-sensing probe, required to make microforce measurements traceable to the SI-units and predicting the corresponding measurement uncertainties, is presented in Table 1. Characteristics such as, a resolution (1σ) of 20 nN given by the standard uncertainty of the signal noise, high selectivity to off-axis forces, defined as the sensor's ability to distinguish the primary input from a parasitic input [31], parallel motion when deflected, and the long sensing probe make this micro force sensing probe an ideal candidate for micromechanical testing of plant cells.

3. Materials and experimental methods

3.1 System Setup

The goal of this work is to develop a system that will be used to automatically characterize the mechanical properties of living organisms in situ. A flexible system suitable for a wide range

of organisms from the sub-cellular to the whole organ level, with changing and highly diverse morphology is required. Positioning capabilities with milimetric range and nanometric resolution is needed to characterize large areas of an organ, for instance a leaf, and to manipulate and characterize individual cells. The applied loads must be in the microNewton range with nanoNewton resolution.

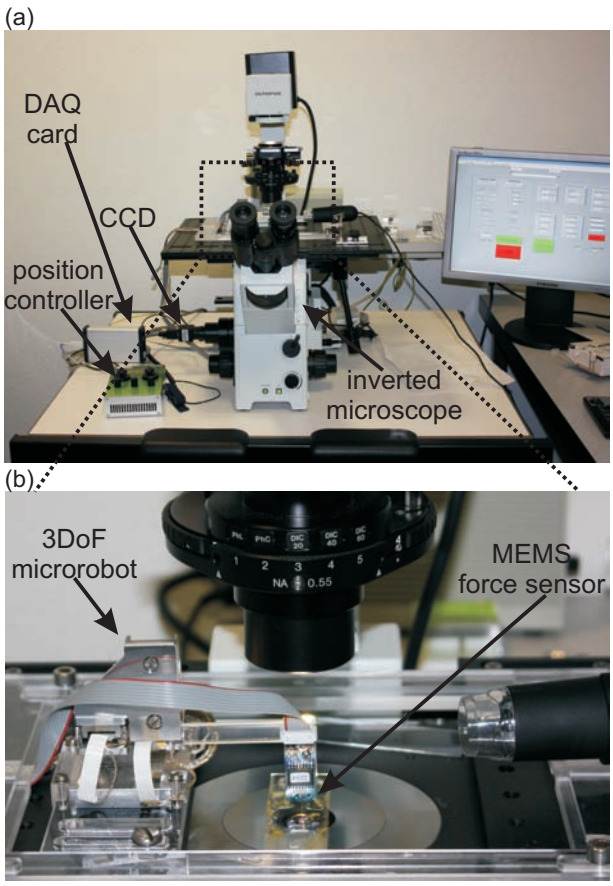

Fig. 5: a) Microrobotic measurement system for mechanical characterization of living cells in situ. b) MEMS force sensor mounted on a 3DoF micropositioning system

To achieve these specifications we designed and developed the experimental setup shown in Fig. 5. The system consists of a MEMS force sensor, a data acquisition system, a three-axis positioning system, a position control unit, a high-resolution optical microscope and custom user interface for the control of automated tasks.

A sharp probe with a 100 nm point radius and 2 mm long was attached to a MEMS capacitive force sensor, FT-S540. The choice of the diameter depends on the properties to be characterized. In this work local elastic properties at subcellular levels are of interest. The force sensor is mounted, as shown in Fig. 5, on a 3DoF positioning system (SmarAct GmbH,

SL-2040) capable of moving over a range of 27 mm with a resolution of 5 nm along each axis. The sensor's end effector is positioned vertically above the glass slide containing the cells to be measured. To ensure that the sensor is perpendicular to the glass slide's surface, a microscope mounted 90 degrees with respect to the sensor (side view) allows for manual alignment.

The imaging system consists of an inverted microscope (Olympus IX 71) with 400X magnification and a CCD camera (Point Grey, Flea 2) that is connected through firewire protocol to a desktop PC. For the acquisition and control of force and position a data acquisition system (National Instruments USB 6009) and a position controller (SmarAct MCS) are needed. These components are integrated with a custom user interface (UI), designed in LabVIEW, into a complete microrobotic measurement system. The UI allows for controlling parameters such as contact/measurement force, speed, step size and measurement locations among others.

Characterization of mechanical properties of the cell wall requires extremely precise manipulation in the nanometer range and, thus, all the parts that comprise the system, apart from the PC, are mounted on a vibration isolation table. In order to avoid noise that stems from the environment, the measurement area is covered with a sealed plexiglass box during experiments.

This system is the first robotic micromechanical system capable of performing highly localized measurements, automated stiffness and/or topography maps of growing cells and structures. The system achieves five nanometers position resolution from integrated encoders and SI-traceable microforce measurements with nanoNewton resolution. The mechanical design and the custom user interface developed offer flexibility for the organism and structure that can be characterized.

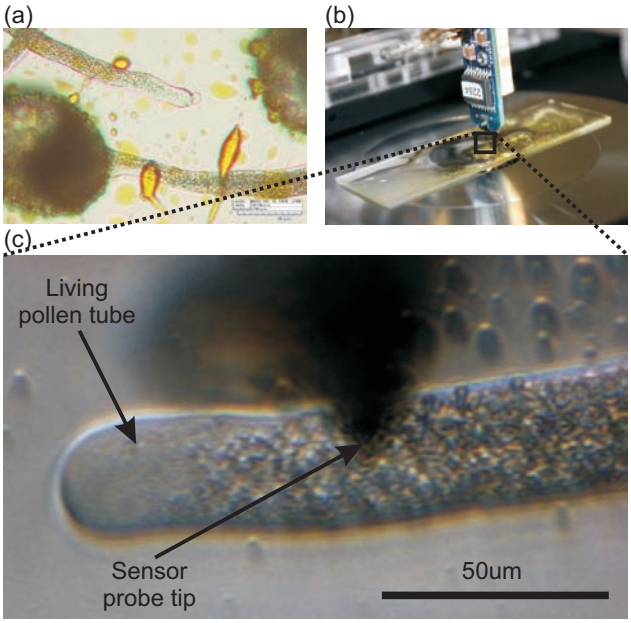

Fig. 6: a) Germinated pollen tubes in growth medium laying on glass slide right before an experiment. b) MEMS force sensor in liquid medium characterizing a living pollen tube. c) Image taken from the inverted microscope during an experiment. The sensor's tip indenting the cell can be seen.

3.2 Pollen Tube preparation

The system was first tested with Lilium longiflorum anthers that were collected three to five days after anthesis, snap-frozen in liquid nitrogen and stored at −80°C for further use. For properly measuring the cell's local or global properties it is important that the cell is well fixed on the substrate. After extensive testing of commercial as well as custom substrates, it was determined that silane was most suitable for lily pollen tubes.Therefore, pollen was dusted on a silane-coated glass slide (Electron Microscopy Sciences, Cat. #63411-01) for cultivation. After hydration in a humid atmosphere for 30 minutes, pollen was covered with growth medium [1] and the slides were incubated at 22°C for two hours. At this point the germinated pollen tubes grew to 400 and 600 μm long, Fig. 6(a).

3.3 Experimental Procedure

The living pollen tubes lie on a glass slide, covered by a thin film of growth medium as shown in Fig. 6(a-b). First, the user chooses, using feedback from the microscope, a candidate pollen tube that is growing and is well fixed on the glass slide. Secondly, the user guides the

force sensing tip in the field of view of the microscope to the starting point of the experiment. Thirdly, the experimental parameters such as contact force, measurement force, approach speed, indentation speed, size and geometry of the measurement area are set by the user depending on the desired force range and cell morphology. The process is ready and the system starts automatic characterization by microindenting the living cells along the length of the tube, Fig. 6(c).

4. Experimental results

The actuation technology of the microrobot used for the positioning tasks is based on piezoelectric actuators (PEA). Two modes of operation of the microrobot are available, the stick slip actuation principle (stepping mode) and direct control of PEA enlongation (scanning mode). The system conducts contact detection based on force feedback. During this phase the microrobot drives the force sensor towards the sample at a speed of 2.7 um/sec using the stick slip priniciple because it provides a larger range of movement (27 mm) compared to the range of the scanning mode (700 nm). When the force read by the force sensor reaches a threshold force value, Fig. 7(a-b), contact is achieved and the measurement procedure begins.

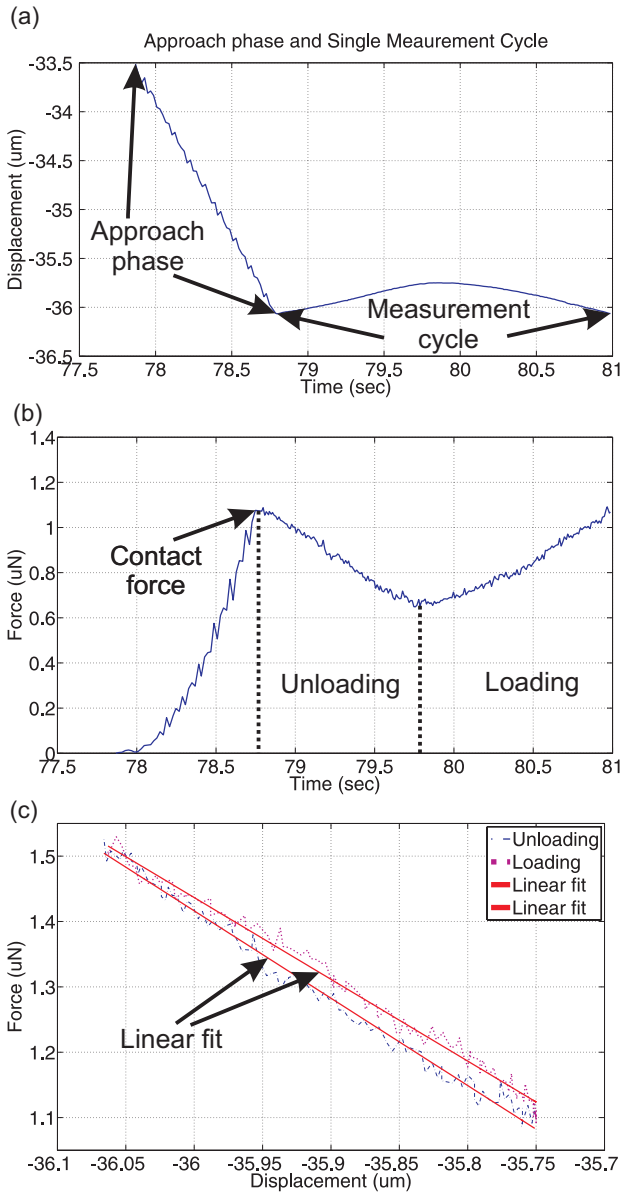

Fig. 7 Experimental data on one pollen tube taken from one measurement point. a) Displacement vs. Time, where the approach and measurement phase are distinguished. b) Force vs. Time for the same data point. c) Force vs Displacement plot used to calculate the observed stiffness by applying linear fit (red lines). The upper dashed curve is the loading phase and the lower is the unloading phase.

To characterize of the cell wall elastic properties, high resolution and fast movements are required. In stepping mode closed-loop motion control, using the integrated position sensors can be performed, achieving steps down to 20 nm, but this requires a 400 msec settling time for each step. In open-loop steps of 50 nm can be achieved but are not always constant due to the stick slip effect. Hence, the microrobot is operated in scanning mode

because it offers continuous movement, in contrast with the discrete steps in stepping mode, and sub-nanometric movement resolution which gives more data points during the 300 nm indentation of the tube. The force and position data are sampled at 50Hz for the contact detection and 100Hz during the measurement phase. A contact force threshold of 1.1 μN is set, while for the measurement phase applied loads of 400 nN that indent the cell wall for 300 nm are achieved. On each measurement point a user-defined number of measurement cycles are performed, with each cycle consisting of a loading and an unloading movement, Fig. 7(a-b).

Data was collected from seven different pollen tubes. All the experiments presented in this paper are based on force-feedback and thus the contact as well as the measurement force are user-defined and pre-set. On each pollen twelve points along the longitudinal axis of symmetry were measured. On each point 2.5 measurement cycles were conducted consisting of two loadings and three unloadings, both at a speed of 0.280 um/sec. While a larger number of measurements at each point is desirable, rapid growth rate of the pollen tubes limits the number of measurements.

Table 2: Experimental Parameters used

Contact Force (μN)	1.1
Measurement Force (μN)	0.4
Contact phase speed (μm/sec)	2.7
Measurement phase speed (μm/sec)	0.28
Indentation depth (nm)	300
Scanning range (nm)	700
Mean scanning mode step size (nm)	60
Stepping mode step size (nm)	5
Measurement locations	12

From the collected force-displacement curves, Fig. 7(c), observed mechanical stiffness of the cell wall can be determined. The stiffness reported here is the instantaneous observed stiffness of the organism, depending on the tip geometry, contact angle etc. Given that we have more than one data points, the stiffness is calculated by applying a linear fit on the Force vs Indentation curve of each measurement as seen in Fig 7c. . The displacement that contributes to the cell's stiffness is the pure indentation of the plant cell. However, the displacement we acquire is the one measured from the position sensors of the 3-axis positioning system, which essentially is a combination of the

cell's indentation and the sensor's probe displacement. In paragraph 2 we mentioned that the sensor consists of a movable body with an attached probe suspended by four flexures within an outer frame. Thus, a force applied to the probe in the measurement direction results in a relative motion of the body and the outer frame.

In order to calculate the organism's stiffness solely, we need to find the system's (positioner, sensor, mounting parts, substrate) stiffness and subtract it from the total stiffness. To this end, measurements are conducted with the exact same configuration (sensor, mounting parts, substrate) in the same environmental conditions but without the organism, in order to determine the system's stiffness only. The system's stiffness, which is about 100 N/m, is subtracted and so the organism's stiffness occurs.

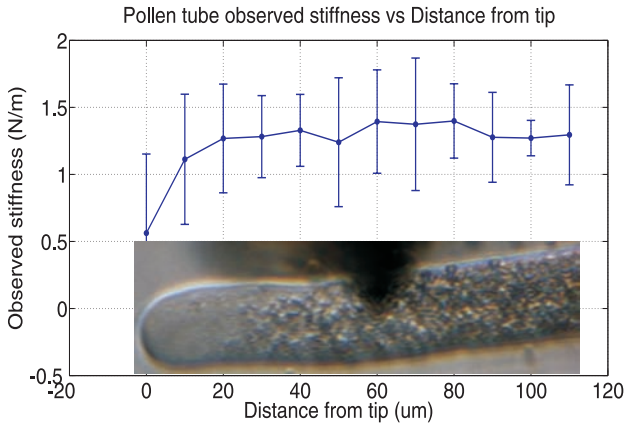

Fig. 8 Observed cell wall stiffness collected from seven pollen tubes. It can be seen that the calculated observed stiffness decreases from the tip to the apex of the cell. The inlet picture depicts a growing Lilium pollen tube along the longitudinal axis of which measurements were conducted.

The average observed stiffness among the seven different pollen tubes on the same glass slide is between 0.5 and 1.5 N/m and is shown in Fig. 8. A difference in the stiffness from the tip to the apex is clearly shown. This finding agrees with the fact that in lily pollen tubes callose is absent from the apical region and pectin is esterified at the tip but not in the shank, which in turn implies that the mechanical properties in the tip and in the shank differ [32,33].

5. Conclusion

To provide biologically plausible models with quantitative data plant growth must be quantitatively studied at cellular, tissue and whole plant levels to enhance the mechanistic understanding of growth-environment interactions. To achieve this, a microrobotic system for the automated mechanical characterization of living plant cells in situ was developed. The system's performance is demonstrated on living lilium pollen tubes for the characterization of their stiffness while they are growing at 20 μm per minute. A MEMS capacitive force sensor with a 100 nm tip radius attached, capable of resolving forces down to 20 nN (1σ, at 10Hz) is used to apply loads of 400 nN. For the positioning tasks a 3 DoF microrobot with sub-nanometer movement resolution is used with integrated optical encoders of 5 nm resolution. The indentation depth applied on the cell wall during the measurements reaches 300 nm. A high-resolution optical microscope is used for providing visual feedback. The force and position control as well as the data acquisition during the automated tasks is performed with a custom designed user interface. Through extensive SI-traceable calibration and characterization with uncertainty analysis, it can be demonstrated that the capacitive microforce sensor is an ideal candidate for micromechanical properties investigation of living plant cells.

The force-displacement curves collected from seven experiments on living pollen tubes show an increase in cell wall stiffness within the first 10 μm from the pollen tube apex. These findings not only verify other research that hypothesizes different mechanical properties between the tip and the shank but also quantifies this difference.

Acknowledgements

This work was financed with a grant from the Swiss SystemsX.ch initiative (SystemsX.ch project: "Plant Growth in a Changing Environment"), evaluated by the Swiss National Science Foundation.

References

1. Zerzour R, Kroeger J, Geitmann A. Polar growth in pollen tubes is associated with spatially confined dynamic changes in cell mechanical properties. Developmental biology. 2009 Oct ;334(2):437-446.

2. Geitmann A. Mechanical modeling and structural analysis of the primary plant cell wall. Current opinion in plant biology. 2010 Oct ;13(6):693-699.

3. Geitmann A, Ortega JKE. Mechanics and modeling of plant cell growth. [Internet]. Trends in plant science. 2009 Sep ;14(9):467-78.

4. Lockhart J a. An analysis of irreversible plant cell elongation. Journal of theoretical biology. 1965 Mar ;8(2):264-275.

5. Cosgrove DJ. Growth of the plant cell wall. Nature reviews. Molecular cell biology. 2005 Nov ;6(11):850-61.

6. Schopfer P. Biomechanics of plant growth. American Journal of Botany. 2006 Oct ;93(10):1415-1425.

7. Zlatanova J, Leuba SH. Magnetic tweezers : a sensitive tool to study DNA and chromatin at the single-molecule level. Biochemistry and Cell Biology. 2003 ;81(3):151-159.

8. Huang C-C, Wang C-F, Mehta DS, Chiou A. Optical tweezers as sub-pico-newton force transducers. Optics Communications. 2001 Aug ;195(1-4):41-48.

9. Ladjal H, Hanus J-L, Pillarisetti A, Keefer C, Ferreira A, Desai JP. Atomic force microscopy-based single-cell indentation: Experimentation and finite element simulation. 2009 IEEE/RSJ International Conference on Intelligent Robots and Systems. 2009 Oct ;1326-1332.

10. Dulinska I, Targosz M, Strojny W, Lekka M, Czuba P, Balwierz W, et al. Stiffness of normal and pathological erythrocytes studied by means of atomic force microscopy. Journal of biochemical and biophysical methods. 2006 Mar ;66(1-3):1-11.

11. Bao G, Suresh S. Cell and molecular mechanics of biological materials. Nature materials. 2003 Nov ;2(11):715-25.

12. Hochmuth RM. Micropipette aspiration of living cells. Journal of biomechanics. 2000 Jan ;33(1):15-22.

13. Kim M-S, Pratt JR. SI traceability: Current status and future trends for forces below 10 microNewtons. Measurement. 2010 Feb ;43(2):169-182.

14. Lin G, Palmer RE, Pister KS, Roos KP. Miniature heart cell force transducer system implemented in MEMS technology. IEEE transactions on bio-medical engineering. 2001 Sep ;48(9):996-1006.

15. Zhang X. J., Zappe S., Bernstein R. W., Sahin O., Chen C. C., Fish M., Scott M., and Solgaard O., Integrated optical diffractive micrograting-based injection force sensor. Transducers: International Conference on Solid-State Sensors, Actuators and Microsystems. 2003 Jun ;1051-1054.

16. Yang S, Saif MT a. Microfabricated Force Sensors and Their Applications in the Study of Cell Mechanical Response. Experimental Mechanics. 2008 Jan ;49(1):135-151.

17. Sun Y, Fry SN, Potasek DP, Bell DJ, Nelson BJ. Characterizing fruit fly flight behavior using a microforce sensor with a new comb-drive configuration. Journal of Microelectromechanical Systems. 2005 Feb ;14(1):4-11.

18. Sun Y, Nelson BJ. Biological Cell Injection Using an Autonomous MicroRobotic System. The International Journal of Robotics Research. 2002 Oct ;21(10-11):861-868.

19. Kim K, Cheng J, Liu Q, Wu XY, Sun Y. Investigation of mechanical properties of soft hydrogel microcapsules in relation to protein delivery using a MEMS force sensor. Journal of biomedical materials research. Part A. 2010 Jan ;92(1):103-13.

20. Beyeler F, Neild A, Oberti S, Bell DJ, Sun Y, Dual J, et al. Monolithically Fabricated Microgripper With Integrated Force Sensor for Manipulating Microobjects and Biological Cells Aligned in an Ultrasonic Field. Journal of Microelectromechanical Systems. 2007 Feb ;16(1):7-15.

21. Muntwyler S, Kratochvil BE, Beyeler F, Nelson BJ. Monolithically Integrated Two-Axis Microtensile Tester for the Mechanical Characterization of Microscopic Samples. Microelectromechanical Systems, Journal of. 2010 ;19(5):1223-1233.

22. Kim K, Liu X, Zhang Y, Sun Y. Nanonewton force-controlled manipulation of biological cells using a monolithic MEMS microgripper with two-axis force feedback. Journal of Micromechanics and Microengineering. 2008 May ;18(5):055013.

23. Benkert R, Obermeyer G, Bentrup F-W. The turgor pressure of growing lily pollen tubes. Protoplasma. 1997 Mar ;198(1-2):1-8. 22.

24. Cardenas L, Lovy-Wheeler A, Kunkel JG, Hepler PK. Pollen tube growth oscillations and intracellular calcium levels are reversibly modulated by actin polymerization. Plant physiology. 2008 Apr ;146(4):1611-21.

25. McKenna ST, Kunkel JG, Bosch M, Rounds CM, Vidali L, Winship LJ, et al. Exocytosis precedes and predicts the increase in growth in oscillating pollen tubes. The Plant cell. 2009 Oct ;21(10):3026-40.

26. Geitmann A, Parre E. The local cytomechanical properties of growing pollen tubes correspond to the axial distribution of structural cellular elements. Sexual Plant Reproduction. 2004 May ;17(1):9-16.

27. Burnham N a, Chen X, Hodges CS, Matei G a, Thoreson EJ, Roberts CJ, et al. Comparison of calibration methods for atomic-force microscopy cantilevers. Nanotechnology. 2003 Jan ;14(1):1-6.

28. Joint Committees for Guides in Metrology. Guide to the expression of uncertainty in measurement. International Organization for Standardization. 2008.

29. Joint Committees for Guides in Metrology. International vocabulary of metrology — Basic and general concepts and associated terms (VIM). International Organization for Standardization. 2007.

30. Joint Committees for Guides in Metrology. Draft: Supplement 2 to the guide to the expression of uncertainty in measurement − Models with any number of output quantities. International Organization for Standardization. 2009.

31. BIPM I, IFCC I, IUPAC I. International Vocabulary of Metrology Basic and General Concepts and Associated Terms (VIM). International Organization for Standardization. 2007:1-127.

32. Taylor LP, Hepler PK. Pollen Germination and Tube Growth. Annual Review of Plant Physiology and Plant Molecular Biology. 1997 ;48(1):461-491.

33. Geitmann A, Parre E. The local cytomechanical properties of growing pollen tubes correspond to the axial distribution of structural cellular elements. Sexual Plant Reproduction. 2004 May ;17(1):9-16.